

Thermoelastic wave induced by pulsed laser heating

X. Wang, X. Xu*

School of Mechanical Engineering, Purdue University, West Lafayette, IN 47907, USA
(Fax: +1-765/494-0539, E-mail: xxu@ecn.purdue.edu)

Received: 23 May 2000/Accepted: 26 May 2000/Published online: 20 September 2000 – © Springer-Verlag 2000

Abstract. In this work, a generalized solution for the thermoelastic plane wave in a semi-infinite solid induced by pulsed laser heating is developed. The solution takes into account the non-Fourier effect in heat conduction and the coupling effect between temperature and strain rate, which play significant roles in ultrashort pulsed laser heating. Based on this solution, calculations are conducted to study stress waves induced by nano-, pico-, and femtosecond laser pulses. It is found that with the same maximum surface temperature increase, a shorter pulsed laser induces a much stronger stress wave. The non-Fourier effect causes a higher surface temperature increase, but a weaker stress wave. Also, for the first time, it is found that a second stress wave is formed and propagates with the same speed as the thermal wave. The surface displacement accompanying thermal expansion shows a substantial time delay to the femtosecond laser pulse. On the contrary, surface displacement and heating occur simultaneously in nano- and picosecond laser heating. In femtosecond laser heating, results show that the coupling effect strongly attenuates the stress wave and extends the duration of the stress wave. This may explain the minimal damage in ultrashort laser materials processing.

PACS: 62.30.+d; 46.40.Cd; 44.10.+i

Excitation of thermoelastic waves by a pulsed laser in solid is of great interest due to extensive applications of pulsed laser technologies in material processing and non-destructive detecting and characterization. When a solid is illuminated with a laser pulse, absorption of the laser pulse results in a localized temperature increase, which in turn causes thermal expansion and generates a thermoelastic wave in the solid. In ultrashort pulsed laser heating, two effects become important. One is the non-Fourier effect in heat conduction which is a modification of the Fourier heat conduction theory to account for the effect

of mean free time (thermal relaxation time) in the energy carrier's collision process. Consideration of the non-Fourier effect also eliminates the paradox of the infinite heat propagation speed [1,2]. The other is dissipation of the stress wave due to coupling between temperature and strain rate, which causes transform of mechanical energy associated with the stress wave to thermal energy of the material.

Many theoretical studies have been conducted to investigate thermoelastic waves. Since numerical techniques, such as the finite element method, do not have sufficient resolution for the thermoelastic wave generated in pulsed laser heating, most work is to search for analytical solutions. Due to the complexity of the generation of thermoelastic waves, various simplifications were used. The simplest approach is to solve thermoelastic wave problems without considering the non-Fourier effect and the coupling effect between temperature and strain rate [3–5]. Welsh et al. [6] solved the two-dimensional thermal stress in a half-space induced by a focused Gaussian beam in the near-surface region. Stress wave propagation and heat conduction in the solid were neglected in his solution.

A large amount of work has been devoted to solving thermoelastic wave problems with the consideration of the coupling effect between temperature and strain rate. Stress waves in a half-space induced by variations of surface strain, temperature, or stress were studied by Boley and Tolins [7], and Chandrasekharaiah and Srinath [8]. Mozina and Dovc [9] attempted to use the Laplace transform to solve the thermoelastic stress wave induced by volumetric heating. Due to the difficulty in finding analytical Green's functions, only the solution for locations far from the surface was obtained.

Research also has been conducted to solve thermoelastic wave problems with the consideration of the non-Fourier effect, but without considering the coupling effect between temperature and strain rate. Kao [10] was the first to investigate the non-Fourier effect on the thermoelastic wave in a half-space. McDonald [11] studied the importance of thermal diffusion on the generation of thermoelastic waves in

*Corresponding author.

metals induced by surface Gaussian laser beam heating. The influence of optical penetration depth and the laser pulse duration on longitudinal acoustic waves induced by volumetric absorption of a laser beam was investigated by Enguehard and Bertrand [12]. The work by Dubois et al. [13] provided detailed information of 3-D thermoelastic waves in an orthotropic medium induced by volumetric absorption of a laser beam.

To solve thermoelastic wave problems in pulsed laser heating, the most complete approach should consider both the non-Fourier effect and the coupling effect. Using this approach, stress waves in a half-space with the simplified boundary condition of step-time variation of strain were studied [14, 15].

The literature discussed above all involves simplification and idealization in either the physical model or the way laser heating is treated. In this work, a generalized solution to the thermoelastic wave in a semi-infinite solid induced by pulsed laser heating is formulated. The solution takes into account the non-Fourier effect in heat conduction, the coupling effect between temperature and strain rate, and the volumetric absorption of laser beam energy. In Sect. 1, the generalized solution to the thermoelastic wave induced by pulsed laser heating is derived. Based on this solution, calculations are conducted and the results are presented in Sect. 2.

1 Theoretical analysis

In this section, solutions to the thermoelastic wave induced by pulsed laser heating are derived. To do so, the laser pulse energy is first represented by Fourier series, and the thermoelastic wave induced by each term in the Fourier series is determined. The summation of Fourier components represents the thermoelastic wave induced by pulsed laser heating. An isotropic, homogeneous solid is assumed to be illuminated with a pulsed laser. The coordinate x is chosen to originate from the surface and pointing towards the inside of the target. The one-dimensional governing equations for the temperature T and the displacement u consist of two coupled equations [8, 14, 16]

$$\frac{\tau_q}{\alpha} \frac{\partial^2 T}{\partial t^2} + \frac{1}{\alpha} \frac{\partial T}{\partial t} = \frac{\partial^2 T}{\partial x^2} + \frac{\beta}{k} (I(t) + \tau_q \dot{I}(t)) e^{-\beta x} - \frac{B\beta_T T_0}{k} \left(\frac{\partial^2 u}{\partial x \partial t} + \tau_q \frac{\partial^3 u}{\partial x \partial t^2} \right), \quad (1a)$$

$$\rho \frac{\partial^2 u}{\partial t^2} = \left(B + \frac{4}{3} G \right) \frac{\partial^2 u}{\partial x^2} - B\beta_T \frac{\partial T}{\partial x}. \quad (1b)$$

In the above equations, $I(t)$ is the intensity of the laser beam, α is the thermal diffusivity, k is the thermal conductivity, ρ is the density, β is the optical absorption coefficient, B and G are the bulk and shear modules of elasticity, β_T is the volumetric thermal expansion coefficient, and T_0 is the initial temperature of the target. τ_q is the thermal relaxation time, which is the mean free time in the energy carrier's collision process and is calculated by dividing the mean free path by the energy carrier's speed [17].

In (1a), the non-Fourier effect term $(\tau_q/\alpha) \partial^2 T/\partial t^2$, along with $\partial^2 T/\partial x^2$, indicate the wave behavior of heat conduction. There are two extra source terms in (1a). One is

$(\beta/k)\tau_q \dot{I}(t) \exp(-\beta x)$, which is induced by the non-Fourier effect, and will only affect the temperature distribution without changing the total energy input to the material since its integration over the whole heating time is zero. The other one is $-(B\beta_T T_0/k)(\partial^2 u/(\partial x \partial t) + \tau_q \partial^3 u/(\partial x \partial t^2))$, which accounts for the transform of mechanical energy to thermal energy. Before heating, the target is assumed to have a uniform temperature, no displacement, and stress free. Also, the first derivatives of temperature and displacement to time are taken as zero. The target surface is assumed to be thermally insulated and stress free, and at $x \rightarrow +\infty$, the target is assumed to have no temperature increase or stress.

By introducing $\theta = T - T_0$, $\gamma = \beta/k$, $\nu = -B\beta_T/(B + 4/3 \times G)$, $c_e = \sqrt{B + 4/3 \times G}/\rho$ and $\varepsilon_T = B\beta_T T_0/k$, (1a) and (1b) can be written in a more concise form

$$\frac{\tau_q}{\alpha} \frac{\partial^2 \theta}{\partial t^2} + \frac{1}{\alpha} \frac{\partial \theta}{\partial t} = \frac{\partial^2 \theta}{\partial x^2} + \gamma (I(t) + \tau_q \dot{I}(t)) e^{-\beta x} - \varepsilon_T \frac{\partial^2 u}{\partial x \partial t} - \varepsilon_T \tau_q \frac{\partial^3 u}{\partial x \partial t^2}, \quad (2a)$$

$$\frac{1}{c_e^2} \frac{\partial^2 u}{\partial t^2} = \frac{\partial^2 u}{\partial x^2} + \nu \frac{\partial \theta}{\partial x}. \quad (2b)$$

The initial and boundary conditions described above are expressed as

$$\theta = 0 \quad \text{at } t = 0, x \geq 0, \quad (3a)$$

$$\frac{\partial \theta}{\partial t} = 0 \quad \text{at } t = 0, x \geq 0, \quad (3b)$$

$$u = 0 \quad \text{at } t = 0, x \geq 0, \quad (3c)$$

$$\frac{\partial u}{\partial t} = 0 \quad \text{at } t = 0, x \geq 0, \quad (3d)$$

$$\frac{\partial \theta}{\partial x} = 0 \quad \text{at } x = 0, t > 0, \quad (3e)$$

$$\frac{\partial u}{\partial x} + \nu \theta = 0 \quad \text{at } x = 0, t > 0. \quad (3f)$$

If laser pulses are periodically fired with a repetition rate f_0 , and the period $p_0 (= 1/f_0)$ is much longer than the laser pulse width, the temperature increase, displacement, and stress wave induced by a single laser pulse are independent of other laser pulses [18, 19]. Therefore, the solutions for periodically fired laser pulses represent the results induced by a single laser pulse.

To solve (2a) and (2b), the laser pulse intensity is represented in terms of Fourier series as

$$I(t) = a_0 + \sum_{i=0}^{\infty} (a_i \cos(i\omega_0 t) + b_i \sin(i\omega_0 t)), \quad (4)$$

where a_0 , a_i , and b_i are coefficients of the Fourier series, and $\omega_0 = 2\pi f_0$. In the solution, only the part that periodically varies with time is of interest, hence, the constant term a_0 in (4) does not need to be considered. Because of the linear relations among θ , u and $I(t)$, as long as the laser beam intensity

is expressed with (4), θ , u , and σ can be written as

$$\theta = \sum_{i=0}^{\infty} (a_i \operatorname{Re}(\tilde{\theta}_i) + b_i \operatorname{Im}(\tilde{\theta}_i)), \quad (5a)$$

$$u = \sum_{i=0}^{\infty} (a_i \operatorname{Re}(\tilde{u}_i) + b_i \operatorname{Im}(\tilde{u}_i)), \quad (5b)$$

$$\sigma = \sum_{i=0}^{\infty} (a_i \operatorname{Re}(\tilde{\sigma}_i) + b_i \operatorname{Im}(\tilde{\sigma}_i)), \quad (5c)$$

where $\tilde{\theta}_i$, \tilde{u}_i , and $\tilde{\sigma}_i$ are the temperature increase, displacement and stress induced by a laser beam with a complex intensity $\exp(j\omega t)$, where j is defined as $\sqrt{-1}$, ω denotes $i\omega_0$, and Re and Im denote the real and imaginary part of a complex number. The resulting governing equations for $\tilde{\theta}_i$ and \tilde{u}_i are

$$\begin{aligned} \frac{\tau_q}{\alpha} \frac{\partial^2 \tilde{\theta}_i}{\partial t^2} + \frac{1}{\alpha} \frac{\partial \tilde{\theta}_i}{\partial t} &= \frac{\partial^2 \tilde{\theta}_i}{\partial x^2} + \gamma(1 + \tau_q j \omega) e^{j\omega t} e^{-\beta x} \\ &\quad - \varepsilon_T \frac{\partial^2 \tilde{u}_i}{\partial x \partial t} - \varepsilon_T \tau_q \frac{\partial^3 \tilde{u}_i}{\partial x \partial t^2}, \end{aligned} \quad (6a)$$

$$\frac{1}{c_e^2} \frac{\partial^2 \tilde{u}_i}{\partial t^2} = \frac{\partial^2 \tilde{u}_i}{\partial x^2} + \nu \frac{\partial \tilde{\theta}_i}{\partial x}. \quad (6b)$$

The boundary conditions are in the same form as (3e) and (3f). The solutions to (6a) and (6b) should have the form of $\tilde{\theta}_i = \theta_i \exp(j\omega t)$ and $\tilde{u}_i = u_i \exp(j\omega t)$ [20, 21]. θ_i and u_i are solved by finding particular solutions:

$$\theta_{p,i} = \frac{s_i e^{-\beta x}}{s_{\theta,i} - \beta^2 + s_{\varepsilon,i} \beta^2 \nu / (\beta^2 + \omega^2 / c_e^2)}, \quad (7a)$$

and

$$u_{p,i} = \frac{s_i \nu \beta e^{-\beta x}}{(s_{\theta,i} - \beta^2)(\beta^2 + \omega^2 / c_e^2) + s_{\varepsilon,i} \beta^2 \nu}, \quad (7b)$$

where $s_i = \gamma(1 + j\omega\tau_q)$, $s_{\varepsilon,i} = (\varepsilon_T \tau_q \omega^2 - \varepsilon_T j \omega)$, and $s_{\theta,i} = j\omega/\alpha - \tau_q \omega^2/\alpha$, and general homogeneous solutions in the form of $\theta_{g,i} = A_i \exp(k_i x)$ and $u_{g,i} = B_i \exp(k_i x)$. The coefficients A_i and B_i are found from the boundary condition. The final solution can be written as

$$\theta_i = A_{1,i} e^{k_{1,i} x} + A_{2,i} e^{k_{2,i} x} + \theta_{p,i}, \quad (8a)$$

$$u_i = -\frac{\nu k_{1,i} A_{1,i}}{\omega^2 / c_e^2 + k_{1,i}^2} e^{k_{1,i} x} - \frac{\nu k_{2,i} A_{2,i}}{\omega^2 / c_e^2 + k_{2,i}^2} e^{k_{2,i} x} + u_{p,i}, \quad (8b)$$

where

$$k_i^2 = \frac{s_{\varepsilon,i} \nu + s_{\theta,i} - \omega^2 / c_e^2}{2} \pm \frac{\sqrt{(s_{\varepsilon,i} \nu + s_{\theta,i} - \omega^2 / c_e^2)^2 + 4s_{\theta,i} \omega^2 / c_e^2}}{2}, \quad (9a)$$

$$A_{1,i} = \frac{\beta A_{p,i} p_{2,i} - p_{3,i} k_{2,i}}{k_{1,i} p_{2,i} - k_{2,i} p_{1,i}}, \quad (9b)$$

$$A_{2,i} = \frac{k_{1,i} p_{3,i} - p_{1,i} \beta A_{p,i}}{k_{1,i} p_{2,i} - k_{2,i} p_{1,i}}. \quad (9c)$$

$p_{m,i}$ is defined as $p_{m,i} = -\nu k_{m,i}^2 / (\omega^2 / c_e^2 + k_{m,i}^2) + \nu$, for $m = 1, 2$ and $p_{3,i} = B_{p,i} \beta - \nu A_{p,i}$.

After θ_i and u_i are obtained, the stress field can be calculated as

$$\sigma_i = \left(B + \frac{4}{3} G \right) \frac{\partial u_i}{\partial x} - B \beta_T \theta_i. \quad (10)$$

$\tilde{\theta}_i$, \tilde{u}_i , and $\tilde{\sigma}_i$ can be obtained by multiplying θ_i , u_i , and σ_i with $\exp(j\omega t)$. The solutions to (2a) and (2b), as well as the stress, can then be calculated using (5a)–(5c).

2 Calculation results and discussions

Based on the solutions derived in Sect. 1, calculations are carried out to investigate thermoelastic waves induced by different laser parameters. The influence of the non-Fourier effect on thermoelastic waves, as well as dissipation of thermoelastic waves due to the coupling effect between temperature and strain rate are studied.

2.1 Ni illuminated with a nanosecond Nd:YLF pulsed laser

In this calculation, Ni is assumed to be the target material illuminated with a nanosecond Nd:YLF pulsed laser at a wavelength of 1.047 μm . The shape of the laser pulse, which is measured using a photo diode, is shown in Fig. 1. The peak laser intensity is taken as $3.065 \times 10^{11} \text{ W/m}^2$, which raises the temperature of the target surface close to the melting point, 1728 K. The thermal relaxation time of Ni is on the order of 1 ps [22], which is much shorter than the laser pulse width. Therefore, the non-Fourier effect is negligible, and is not considered in this calculation. Due to the relatively long heating time of the ns Nd:YLF pulsed laser, the thermoelastic wave has a low strain rate, resulting a negligible coupling effect. Therefore, the coupling effect is not considered in this calculation either. Properties of Ni used in the calculation are listed in Table 1 [23–25].

Figure 2 shows the temperature increase and displacement at the surface. It reveals that when the temperature increases, the displacement of the surface also increases. At $x \rightarrow +\infty$, the target is assumed fixed. Therefore, the laser heating induced thermal expansion causes the target surface to move in the $-x$ direction, resulting in a negative surface displacement. Figure 3 shows how the stress wave is

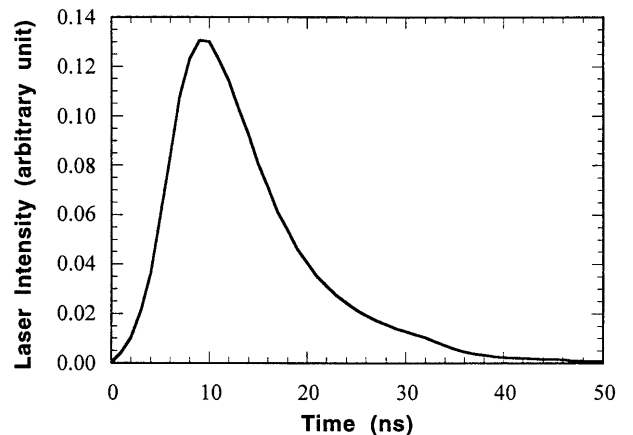
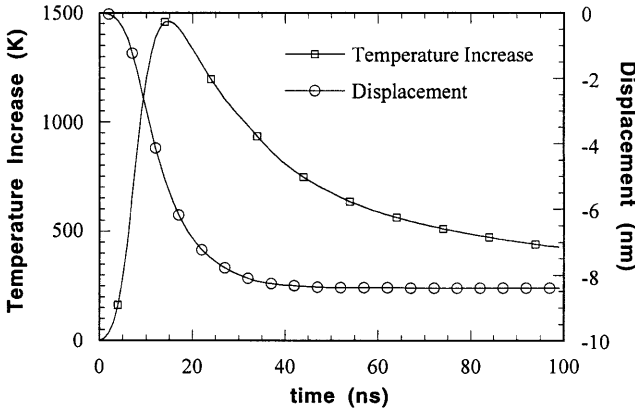
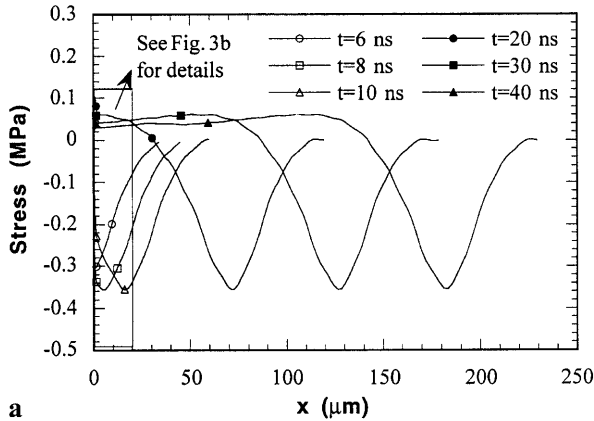


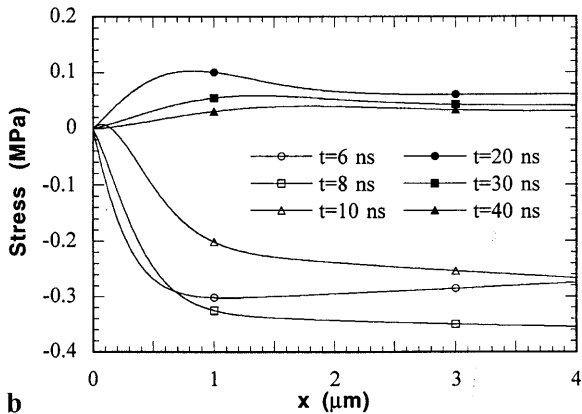
Fig. 1. Shape of the laser pulse generated by a ns Nd:YLF laser

Table 1. Properties of nickel used in the calculation

Property	Value
ρ , density (kg/m ³)	8.9×10^3
k , thermal conductivity (W/m K)	90.7
c_p , specific heat (J/kg K)	4.44×10^2
β , optical absorption coefficient (1/m)	6.175×10^7
G , shear modulus (kg/s ² m)	7.584×10^{10}
B , bulk modulus (kg/s ² m)	1.72×10^{11}
β_T , volumetric thermal expansion coefficient (1/K)	1.26×10^{-5}

**Fig. 2.** Temperature increase and displacement at the surface of Ni illuminated with a ns Nd:YLF laser

a



b

Fig. 3. Stress waves at different times in Ni illuminated with a ns Nd:YLF laser

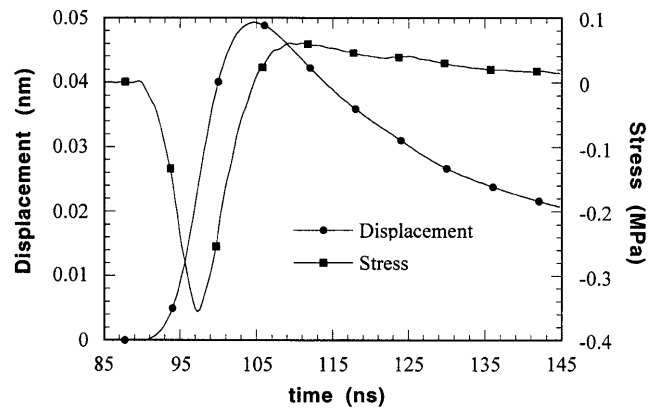
generated from the surface and propagates into the target. It is seen from Fig. 3 that after about 10 ns, the compressive stress reaches its peak value and stays as a constant. Details of the stress development in the near-surface region are indicated in Fig. 3b, which shows a change from compression to tension during the initial tens of ns. Figure 4 shows the displacement and stress waves at the location of 0.5 mm from the surface. The front of the displacement wave increases sharply but its tail decreases slowly, causing a high compressive stress and a low tensile stress. Comparing Fig. 4 with Fig. 2, it is seen that the amplitude of the displacement wave at 0.5 mm is much smaller than the surface displacement.

2.2 Ni illuminated with a picosecond pulsed laser

In this problem, a nickel target is illuminated with a ps pulsed laser having a wavelength of 0.8 μm , a triangular pulse shape with a pulse width of 50 ps, and a peak intensity of $9.6 \times 10^{12} \text{ W/m}^2$ in the middle of the pulse. Properties of nickel are the same as those listed in Table 1, except the optical absorption coefficient, which is taken as $6.757 \times 10^7 \text{ m}^{-1}$ instead of $6.175 \times 10^7 \text{ m}^{-1}$ since the laser beam is assumed to have a wavelength of a Ti:sapphire pico- and femtosecond laser. Since the thermal relaxation time of nickel is not known exactly, several different thermal relaxation times are used in the calculation to study the influence of the thermal relaxation time on temperature and thermoelastic waves.

Calculations are first conducted to investigate the influence of the non-Fourier effect on the behavior of heat transfer and thermoelastic waves with different thermal relaxation times. For simplicity, the coupling effect between the temperature and the strain rate is not taken into account and will be considered later. Shown in Fig. 5a is the variation of the surface temperature increase with different thermal relaxation times. It is seen from Fig. 5a that a larger thermal relaxation time causes a higher surface temperature increase. This is because a larger thermal relaxation time causes a slower heat propagation speed ($= \sqrt{\alpha/\tau_q}$ as seen from (1a)), therefore, more heat is accumulated near the surface.

Total surface displacements are almost the same, which are shown in Fig. 5b.

**Fig. 4.** Displacement and stress as a function of time at the location of 0.5 mm in Ni illuminated with a ns Nd:YLF laser

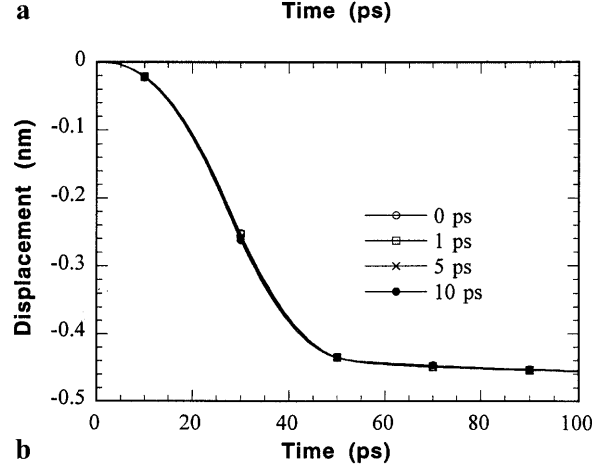
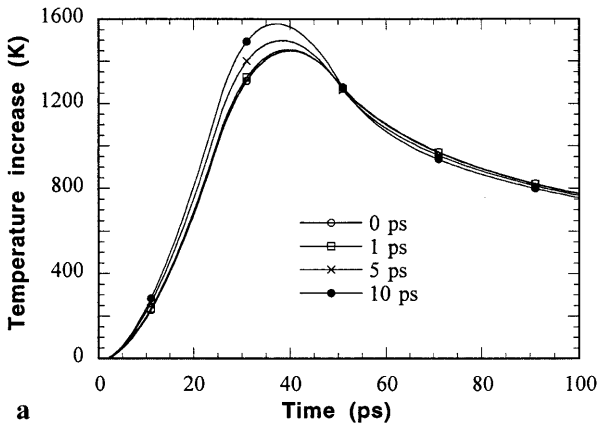


Fig. 5. **a** Variation of surface temperature increase, and **b** variation of surface displacement with different thermal relaxation times in Ni illuminated with a ps laser

Figure 6a shows the displacement as a function of time at the location of 0.3 mm from the surface. From this figure, it is found that the displacement with a larger thermal relaxation time has a smaller amplitude, which induces a weaker stress as shown in Fig. 6b. It is seen from Fig. 6b that the amplitude of the stress wave with a thermal relaxation time of 10 ps is noticeably smaller than that without considering the non-Fourier effect. Comparing Fig. 6 with Fig. 4, it is seen that with the same maximum surface temperature increase, the ps laser induces much stronger displacement and stress wave than the ns laser does.

Figure 7a shows the temperature distribution inside the target at different times with a thermal relaxation time of 10 ps. With a non-zero thermal relaxation time, a thermal wave should be formed. This thermal wave is not clearly seen in the temperature profiles indicated in Fig. 7a. However, the stress wave induced by the thermal wave, called the second stress wave here, can be seen in Fig. 7b. This second stress wave is damped away quickly because of dissipation of the thermal wave. It is seen that at 200 ps, the second stress wave has mostly disappeared. In the calculation, it is also found that with a smaller thermal relaxation time, the temperature and the second stress waves become less obvious and are damped away within a shorter distance from the surface.

When the coupling effect between temperature and strain rate is considered, the temperature increase and the displace-

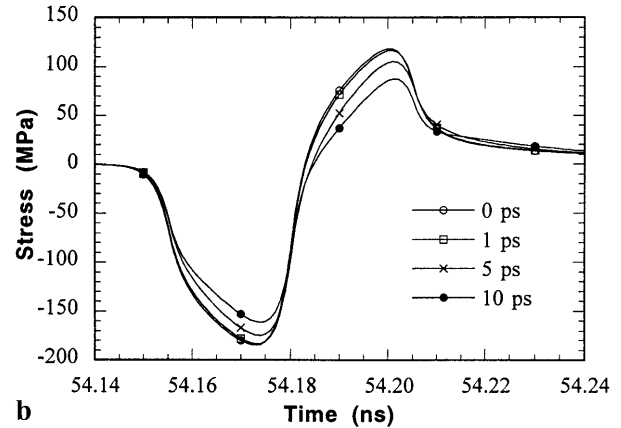
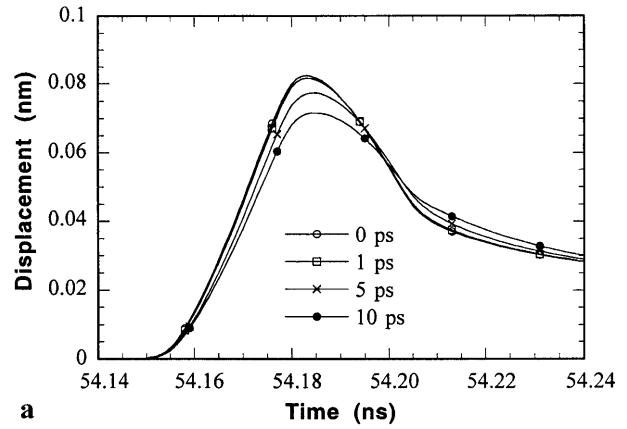


Fig. 6. **a** Displacement, and **b** stress as a function of time at the location of 0.3 mm with different thermal relaxation times in Ni illuminated with a ps laser

ment at the surface show little difference in comparison with results without considering the coupling effect. Figure 8a shows the time evolution of stress waves in the near-surface region. From Fig. 8b, it is seen that the amplitude of the stress waves is damped quickly as the stress wave propagates away from the surface.

2.3 Ni illuminated with a femtosecond pulsed laser

In this case nickel is illuminated with a fs pulsed laser, which has a wavelength of 0.8 μm , a base pulse width of 200 fs, and a peak intensity of $9.502 \times 10^{14} \text{ W/m}^2$. This laser intensity is chosen to cause the same maximum surface temperature increase as those in ns and ps laser cases discussed previously. The thermal relaxation time of nickel is chosen to be 1 ps.

The influence of the non-Fourier effect on heat transfer and the thermoelastic wave is studied first. For simplicity, the coupling effect is not taken into account but will be considered later. Figure 9 shows the temperature increase and the displacement at the surface. Unlike the displacement induced by ns or ps laser heating, during fs laser heating, the surface displacement does not respond to the laser pulse immediately. From Figs. 2 and 5, it is seen that for ns and ps laser heating, the surface displacement reaches its maximum value at the end of the laser pulse. On the other hand, it is seen from Fig. 9 that after the fs laser pulse stops, the surface displacement is relatively small in

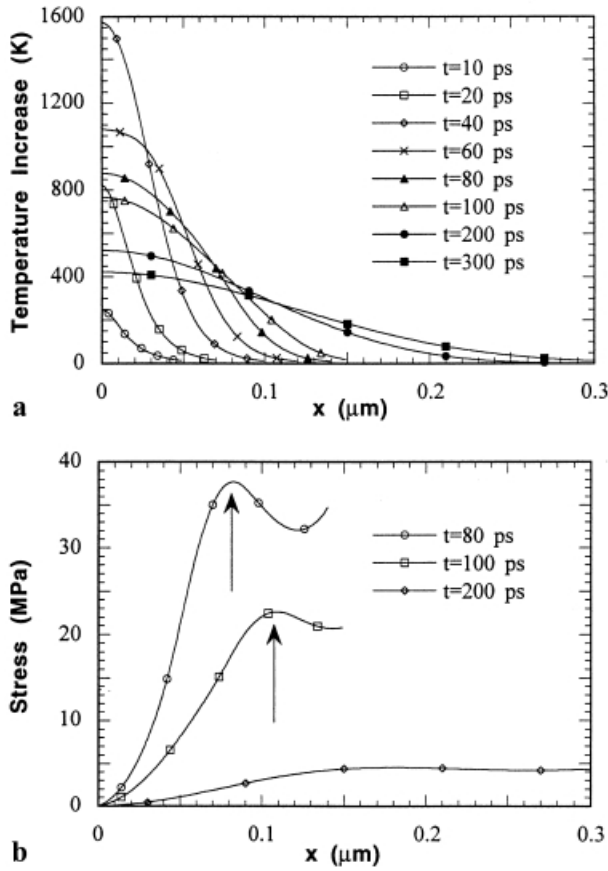


Fig. 7. **a** Temperature distribution, and **b** the second stress wave at different times in Ni illuminated with a ps laser. $\tau_q = 10$ ps

comparison with the final surface displacement. The surface displacement does not reach its maximum value until 20 ps. This is because during fs laser heating, it takes some time for the thermal expansion of the inner material to reach the surface. On the other hand, this time is small compared with ns and ps laser pulse width, therefore, the time delay is not observed in ns and ps laser heating.

Compared with the results in ps laser heating, the non-Fourier effect in fs laser heating causes a larger temperature difference compared with that without the non-Fourier effect. On the other hand, this surface temperature difference causes little difference in the surface displacement as indicated in Fig. 9.

Figure 10 shows the displacement and the stress wave at the location of 0.3 mm from the surface. Several features can be observed from Fig. 10. First, the stress wave lasts about 20 ps, much longer than the laser pulse width. Note that in ns and ps laser heating, the stress wave has the same duration as that of the laser pulse (Figs. 4 and 6). From Fig. 9, it is seen that the surface displacement keeps decreasing within the first 20 ps, which explains the prolonged stress wave inside the target. Second, the stress wave has a different waveform from the ones induced by ns or ps laser heating. A smooth wave front followed by a sharp stress jump is observed in fs laser heating. Last, the amplitude of the displacement is comparable to the surface displacement variation, whereas in ns and ps laser heating,

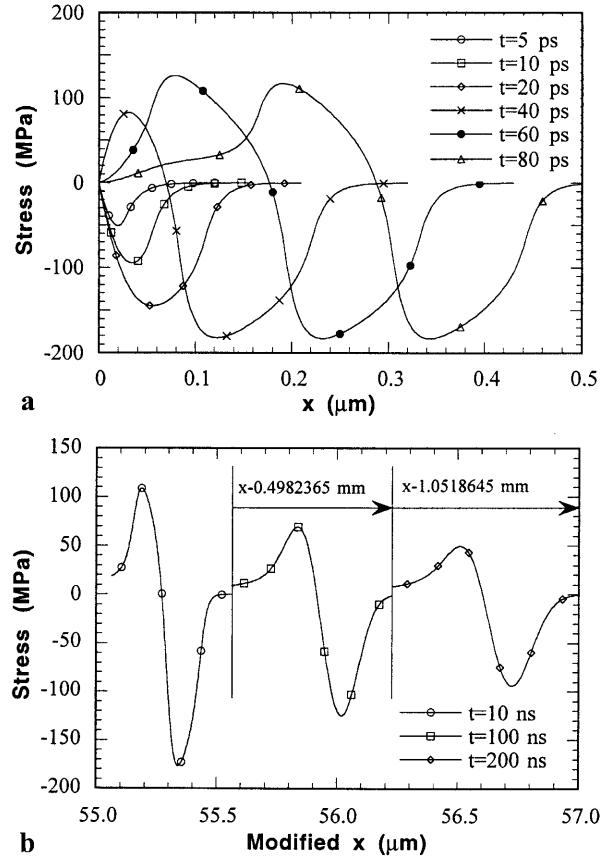


Fig. 8. Stress waves at different times in Ni illuminated with a ps laser. $\tau_q = 1$ ps, and the coupling effect is considered

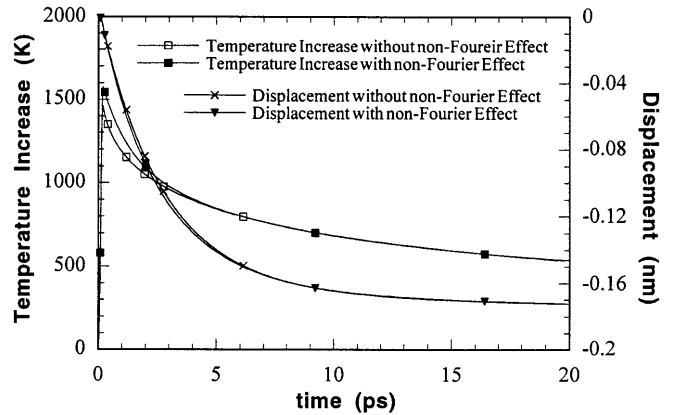


Fig. 9. Temperature increase and displacement as a function of time at the surface of Ni illuminated with a fs laser. $\tau_q = 1$ ps

the amplitude of the displacement wave is much smaller than the surface displacement. The amplitude of the displacement induced by fs laser heating is about 30% larger than that induced by ps laser heating, and the stress is an order of magnitude higher.

When the coupling effect is considered, the temperature increase and the displacement at the nickel surface show little difference in comparison with the results without considering the coupling effect. Figure 11 shows the time evolution of the temperature distribution in the near-surface region.

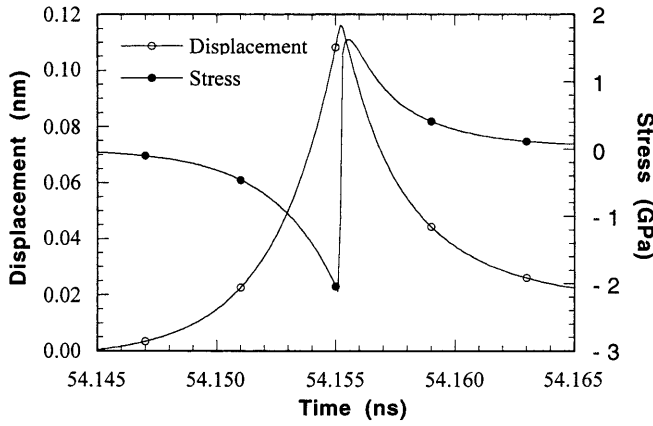


Fig. 10. Displacement and stress waves at the location of 0.3 mm in Ni illuminated with a fs laser. $\tau_q = 1$ ps

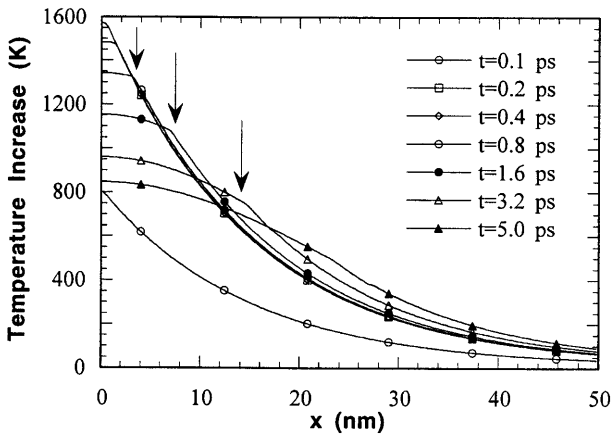


Fig. 11. Temperature increase at different times in Ni illuminated with a fs laser. $\tau_q = 1$ ps, and the coupling effect is considered

The sharp temperature decreases marked by the arrows result from the thermal wave effect. This wave is quickly dissipated as it propagates into the material. Shown in Fig. 12 is how the stress wave develops. It is seen from Fig. 12a that within about 50 nm from the surface, the stress wave is completely developed. Damping of the stress wave during its propagation is shown in Fig. 12b. It is seen that after 20 ns, the stress wave is damped by one order of magnitude. This damping is much stronger than that in ps laser heating.

The above calculations provide detailed pictures of thermoelastic waves induced by ns, ps, and fs pulsed laser heating. However, there are several limiting factors in these calculations. First, for ultrafast laser heating, the solution developed in this work is more suitable for thermoelastic waves in dielectric materials although nickel is used in calculations. For metals illuminated with ultrafast pulsed lasers, the two-step model which accounts for the non-equilibrium between electrons and the lattice should be applied [26], in which the electrons absorb the photon energy first, then transfer it to the lattice. The method used to derive the above solutions also can be extended to include the two-step model. Work is in progress to develop the solution based on the two-step model. Another limiting factor is that thermophysical properties of

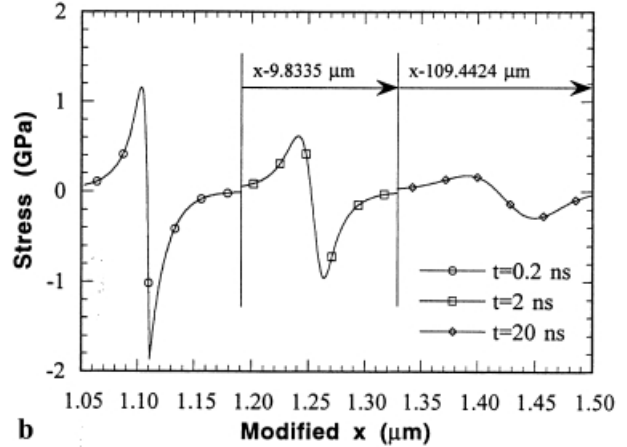
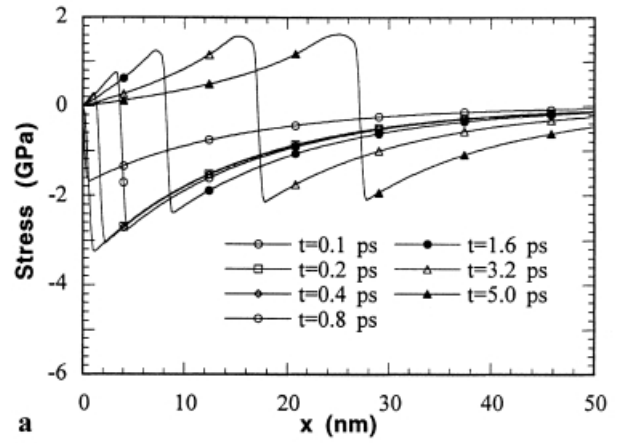


Fig. 12. Stress waves at different times in Ni illuminated with a fs laser. $\tau_q = 1$ ps, and the coupling effect is considered

the target are treated as constants despite the fact that they are temperature dependent. Nevertheless, the results are still useful to illustrate the fundamental characteristics of heat transfer and thermoelastic waves in pulsed laser heating.

3 Conclusion

In this work, a generalized solution is derived for thermoelastic waves in a solid induced by pulsed laser heating. The non-Fourier effect in heat conduction, the coupling effect between temperature and strain rate, and the volumetric absorption of laser beam energy are all considered. Calculations are carried out to provide detailed information of pulsed-laser-induced thermoelastic waves. The results lead to the following conclusions. First, it is found that with the same maximum surface temperature increase, a shorter pulsed laser induces a much stronger stress wave. Second, the non-Fourier effect induces a higher surface temperature increase, but a weaker stress wave. Third, a second stress wave is observed due to the thermal wave caused by the non-Fourier effect. The fourth observation is that in fs laser heating, the surface displacement has a substantial time delay to the laser pulse. Last, the coupling effect between temperature and strain rate damps the amplitude of the stress waves and extends the duration of the stress waves during their propagation in the space.

Acknowledgements. Support for this work by the National Science Foundation (CTS-9624890) is gratefully acknowledged.

References

1. D.D. Joseph, L. Preziosi: *Rev. Mod. Phys.* **61**, 41 (1989)
2. D.D. Joseph, L. Preziosi: *Rev. Mod. Phys.* **62**, 375 (1990)
3. R.M. White: *J. Appl. Phys.* **34**, 3559 (1963)
4. J.C. Bushnell, D.J. McCloskey: *J. Appl. Phys.* **39**, 5541 (1968)
5. A. Galka, R. Wojnar: *J. Therm. Stress* **18**, 113 (1995)
6. L.P. Welsh, J.A. Tuchman, I.P. Herman: *J. Appl. Phys.* **64**, 6274 (1988)
7. B.A. Boley, I.S. Tolins: *J. Appl. Mech.* **29**, 637 (1962)
8. D.S. Chandrasekharaiah, K.S. Srinath: *J. Thermal Stress* **20**, 659 (1997)
9. J. Mozina, M. Dovc: *Mod. Phys. Lett. B* **8**, 1791 (1994)
10. T.T. Kao: *AIAA Journal* **14**, 818 (1976)
11. F.A. McDonald: *Appl. Phys. Lett.* **56**, 230 (1990)
12. F. Enguehard, L. Bertrand: *J. Appl. Phys.* **82**, 1532 (1997)
13. M. Dubois, F. Enguehard, L. Bertrand, M. Choquet, J.P. Monchalain: *Appl. Phys. Lett.* **64**, 554 (1994)
14. H.W. Lord, Y. Shulman: *J. Mech. Phys. Solids* **15**, 299 (1967)
15. D.W. Tang, N. Araki: *Proceedings of the Second International Conference on Stresses and Related Topics*, 657 (1997)
16. D.W. Tang, N. Araki: *Heat Mass Transfer* **31**, 359 (1996)
17. D.Y. Tzou: *Macro- to Microscale Heat Transfer — The Lagging Behavior* (Taylor and Francis, Washington 1996)
18. C. Thomsen, H.T. Grahn, H.J. Maris, J. Tauc: *Phys. Rev. B* **34**, 4129 (1986)
19. B. Bonello, B. Perrin, E. Romatet, J.C. Jeannet: *Ultrasonics* **35**, 223 (1997)
20. F.A. McDonald, G.C. Wetsel: *J. Appl. Phys.* **49**, 2313 (1978)
21. P.M. Morse, K.U. Ingard: *Theoretical Acoustics* (Princeton University Press, Princeton, NJ 1986)
22. A. Vedavarz, S. Kumar, M.K. Moallemi: *Winter Annual Meeting of the American Society of Mechanical Engineers. DSC* **32**, 109 (1991)
23. F.P. Incropera, D.P. DeWitt: *Fundamentals of Heat and Mass Transfer*, 4th edn. (Wiley, New York 1996)
24. D.R. Lide: *CRC Handbook of Chemistry and Physics: A Ready-reference Book of Chemical and Physical Data* (CRC Press, Boca Raton, FL 1994)
25. S.P. Marsh: *Shock Hugoniot Data* (University of California Press, Berkeley, CA 1980)
26. T.T. Qiu, C.L. Tien: *J. Heat Transfer* **115**, 835 (1993)